Clinical Chemistry 62:9
1238–1247 (2016)

Multiplex Droplet Digital PCR Quantification of Recurrent Somatic Mutations in Diffuse Large B-Cell and Follicular Lymphoma

Miguel Alcaide,[1] Stephen Yu,[1] Kevin Bushell,[1] Daniel Fornika,[1] Julie S. Nielsen,[2] Brad H. Nelson,[2] Koren K. Mann,[3] Sarit Assouline,[3] Nathalie A. Johnson,[3] and Ryan D. Morin[1,4*]

BACKGROUND: A plethora of options to detect mutations in tumor-derived DNA currently exist but each suffers limitations in analytical sensitivity, cost, or scalability. Droplet digital PCR (ddPCR) is an appealing technology for detecting the presence of specific mutations based on a priori knowledge and can be applied to tumor biopsies, including formalin-fixed paraffin embedded (FFPE) tissues. More recently, ddPCR has gained popularity in its utility in quantifying circulating tumor DNA.

METHODS: We have developed a suite of novel ddPCR assays for detecting recurrent mutations that are prevalent in common B-cell non-Hodgkin lymphomas (NHLs), including diffuse large B-cell lymphoma, follicular lymphoma, and lymphoplasmacytic lymphoma. These assays allowed the differentiation and counting of mutant and wild-type molecules using one single hydrolysis probe. We also implemented multiplexing that allowed the simultaneous detection of distinct mutations and an "inverted" ddPCR assay design, based on employing probes matching wild-type alleles, capable of detecting the presence of multiple single nucleotide polymorphisms.

RESULTS: The assays successfully detected and quantified somatic mutations commonly affecting enhancer of zeste 2 polycomb repressive complex 2 subunit (*EZH2*) (Y641) and signal transducer and activator of transcription 6 (*STAT6*) (D419) hotspots in fresh tumor, FFPE, and liquid biopsies. The "inverted" ddPCR approach effectively reported any single nucleotide variant affecting either of these 2 hotspots as well. Finally, we could effectively multiplex hydrolysis probes targeting 2 additional lymphoma-related hotspots: myeloid differentiation primary response 88 (*MYD88*; L265P) and cyclin D3 (*CCND3*; I290R).

CONCLUSIONS: Our suite of ddPCR assays provides sufficient analytical sensitivity and specificity for either the invasive or noninvasive detection of multiple recurrent somatic mutations in B-cell NHLs.

Quantification of circulating tumor DNA (ctDNA)[5] in plasma from cancer patients has recently emerged as a powerful and noninvasive method to monitor tumor burden in solid cancers including non-Hodgkin lymphomas (NHLs) *(1)*. Assays for quantifying ctDNA in NHLs thus far have leveraged the presence of clonal structural alterations characteristic of mature B cells *(2)*. Although these demonstrate promise for tracking tumor burden and measuring minimal residual disease with exquisite analytical sensitivity, such methods are blind to the somatic driver mutations in the tumor. A clear benefit of detecting such mutations extends so-called "liquid biopsy" approaches beyond simple monitoring to the appealing potential of prognostication and informing on therapeutic management *(3, 4)*. For instance, the noninvasive assessment of recurrent KRAS proto-oncogene, GTPase (*KRAS*)[6] mutations in metastatic colorectal and other cancers has attracted attention given their involvement in innate and acquired resistance to standard therapeutic treatments *(5, 6)*.

Mutations with potential diagnostic or prognostic implications have begun to emerge from common NHLs *(7)*. For example, somatic mutations affecting the residue Y641 of the enhancer of zeste 2 polycomb repressive complex 2 subunit (*EZH2*) histone methyltransferase have been identified in more than 20% of cases of the germinal

[1] Department of Molecular Biology and Biochemistry, Simon Fraser University, Burnaby, BC, Canada; [2] Deeley Research Centre, BC Cancer Agency, Victoria, BC, Canada; [3] Department of Medicine, Jewish General Hospital, Montreal, Quebec, Canada; [4] Genome Sciences Centre, BC Cancer Agency, Vancouver, BC, Canada.
* Address correspondence to this author at: Department of Molecular Biology and Biochemistry, Simon Fraser University, 8888 University Drive, 7157 SSB, Burnaby, BC, Canada, V5A 1S6. Fax 778-782-9582; e-mail rdmorin@sfu.ca.
Received January 27, 2016; accepted June 23, 2016.
Previously published online at DOI: 10.1373/clinchem.2016.255315

[5] Nonstandard abbreviations: ctDNA, circulating tumor DNA; NHL, non-Hodgkin lymphoma; DLBCL, diffuse large B-cell lymphoma; ddPCR, droplet digital PCR; FFPE, formalin-fixed paraffin embedded; VAF, variant allele frequency.
[6] Human genes: *KRAS,* KRAS proto-oncogene, GTPase; *EZH2,* enhancer of zeste 2 polycomb repressive complex 2 subunit; *STAT6,* signal transducer and activator of transcription 6; *MYD88,* myeloid differentiation primary response 88; *CD79B,* CD79b molecule; *CCND3,* cyclin D3; *ALK,* anaplastic lymphoma receptor tyrosine kinase; *ROS1,* ROS proto-oncogene 1, receptor tyrosine kinase; *RET,* ret proto-oncogene; *BRAF,* B-Raf proto-oncogene, serine/threonine kinase; EGFR, epidermal growth factor receptor.

center B-cell molecular subtype of diffuse large B-cell lymphoma (DLBCL) and follicular lymphoma tumors *(8, 9)*. Owing to the functional effect of this mutation on the catalytic activity of the Polycomb Repressive Complex 2, *EZH2*-driven lymphomas are generally considered to have increased trimethylation activity of histone H3 on K27. As a result, research efforts have been aimed at the design of small pharmacological inhibitors of the *EZH2* catalytic subunit in these cancer types *(10, 11)* and potential therapeutic inhibitors developed for treating *EZH2*-driven cancers have entered clinical trials. Likewise, mutations affecting the residue D419 of the transcription factor signal transducer and activator of transcription 6 (*STAT6*) have been detected in more than 10% of follicular lymphoma cases *(12)* and have recently been associated with therapeutic resistance and relapse in DLBCLs *(13)*. Here, recurrent D419 mutations were observed in 36% of relapsed/refractory germinal center B-cell–DLBCL cases and linked to increased expression of *STAT6* targets. Each of these genes bears a mutation "hotspot" at the affected codon with 4 commonly observed alleles. Additional recurrently mutated genes are also characterized by mutation hotspots in B-cell lymphomas, including myeloid differentiation primary response 88 (*MYD88*; L265P), CD79b molecule (*CD79B*; Y196C), or cyclin D3 (*CCND3*; I290R) *(13–15)*. *MYD88* mutations are found in most cases of lymphoplasmacytic lymphoma *(16)*, and both *MYD88* and *CD79B* mutations are common in the more aggressive activated B-cell molecular subtype of DLBCL. Such mutations are associated with new therapeutics that inhibit oncogenic pathways driving these tumors and may be considered as potentially predictive or prognostic biomarkers *(17, 18)*. Given the noninvasive potential for screening plasma samples for tumor-associated mutations, there is considerable interest in developing liquid biopsies to identify such mutations not only for informing patients on treatment options but also as a potential method for measuring tumor dynamics.

Regardless of whether the genetic profiling of patients is accomplished via invasive tumor biopsies *(13, 19)* or through more attractive noninvasive methods *(1, 3–4)*, there is an unmet need for accurate and cost-effective assays to screen for the presence of cancer-related genetic aberrations. Monitoring ctDNA in plasma has major clinical advantages over needle core biopsies, including reduced morbidity, faster turnaround times, and the possibility to detect subclonal mutations that may be overlooked in traditional biopsies because of tumor heterogeneity *(20)*. Allele-specific assays and assays with high analytical sensitivity, relying on hydrolysis probes, have proven successful in the detection and quantification of single nucleotide polymorphisms *(6)*, indels *(21)*, copy number changes *(22)*, and structural variants *(23, 24)*. Even the most robust of these assays nonetheless suffer limitations for screening applications. One key limitation is the requirement for multiple probes to cover the full spectrum of known mutations at a hotspot. Few studies have satisfactorily designed such multiplexed assays *(6)* and, because there is no guarantee that any given pool of probes detects the presence of all possible mutant alleles *(25)*, there is a risk of false negatives associated with such assays. Because ctDNA can be present at levels as low as 1 mutant copy per 10 000 wild-type copies during initial or residual stages of the disease *(1, 3–4)*, or in cancers affecting the central nervous system *(26)*, conventional PCR-based methods do not offer enough analytical sensitivity *(27–29)*. Nevertheless, droplet digital PCR (ddPCR) has fuelled powerful approaches for the absolute quantification of ctDNA, holding promise for the early detection and more comprehensive monitoring of cancer malignancies *(30–32)*.

The use of molecular probes in ddPCR enables the parallel compartmentalization, replication, and detection of single DNA molecules in thousands of droplets of nanoliter volumes. This technology also offers the possibility to leverage differences in probe concentration to generate different fluorescence amplitude bands, affording the simultaneous assessment of several mutations *(6)*. Here, we describe a suite of ddPCR assays for detecting and quantifying clinically relevant *EZH2, STAT6*, *MYD88*, and *CCND3* mutations in B-cell lymphomas.

Methods

SAMPLE ACQUISITION

Genomic DNA from the DLBCL cell lines WSU-DLCL2 and DB were used as controls for the *EZH2* Y641F and Y641N mutations, respectively *(33)*. Cell line DNA was sheared to approximately 200 bp using a Covaris M220 focused ultrasonicator (Thermo Fisher Scientific) and subjected to a double size selection to mimic cell-free DNA using AMPURE XP beads (Beckman Coulter). We validated our ddPCR assays on a collection of clinical samples with previously known mutations, including fresh (n = 27) and formalin-fixed paraffin embedded (FFPE) (n = 4) tumor biopsies (see Table 1 in the Data Supplement that accompanies the online version of this article at http://www.clinchem.org/content/vol62/issue9). The DNA extracted from fresh tumors was sheared to a mean 300 bp. FFPE samples were processed with the QiAamp DNA FFPE tissue kit (Qiagen). DNA samples were stored at −20 °C in Tris-EDTA buffer for several months *(13, 34)*. Liquid biopsies were also collected within a clinical trial (n = 17) testing the efficacy of the drug Panobinostat (a histone deacetylase inhibitor) *(34)* plus 4 additional plasma samples, 2 from 2 additional DLBCL patients and 2 samples collected from patients with lymphoplasmacytic lymphoma (see online Supplemental Table 1). We used the

QiAamp circulating DNA kit (Qiagen) to extract cfDNA from plasma *(34)*. cfDNA samples were stored in AVE Buffer (Qiagen) at −20 °C during several months. We used a mixture of human genomic DNA (Promega) as a source of wild-type DNA and as negative control during our experiments. Pools of DNA samples known to harbor different mutations were also used during our multiplexed experiments.

PROBE DESIGN AND ddPCR EXPERIMENTS

We designed Custom PrimeTime© Mini LNA probes and ZEN double-quenched hydrolysis probes (Integrated DNA Technologies) for *EZH2* (Y641), *STAT6* (D419), *MYD88* (L265), and *CCND3* (I290) hotspots, as described in the online Supplemental Methods file. Digital PCR reactions were performed in an automated QX200 ddPCR system (Bio-Rad). Each amplification reaction was prepared in a final volume of 20 μL containing 10 μL of 2× ddPCR Supermix for Probes (no dUTP) (Bio-Rad), 1.0–1.125 μmol/L of primers, between 0.015 and 0.5 μmol/L of each corresponding hydrolysis probe for multiplex assays, 0.312 μmol/L of probes or unlabeled competing oligonucleotides (optional) for uniplex or duplex assays. We used a variable amount of input DNA that ranged from 1 to 30 ng, according to Qubit readings (ThermoFisher Scientific). The thermocycling protocol of the nano-droplet emulsion consisted of an initial denaturalization step of 10 min at 95 °C, followed by 39 cycles of 30 s at 94 °C and 1 min at 58 °C (*EZH2* assays) or 60 °C (for the remaining assays) plus a final incubation time of 10 min at 98 °C. Droplets were analyzed in an automated QX200 droplet reader. Multiplexed assays targeting up to 4 variants in both *EZH2* and *STAT6* hotspots relied on the optimization of the concentration of the 4 probes targeting each of the 4 mutant alleles (see online Supplemental Methods file). The fractional abundance of each allele, expressed as variant allele frequency (VAF), was calculated using the QuantaSoft ver 1.7.4 software (Bio-Rad). We found it critical that the right type of ddPCR Supermix and fresh reagents were used. Our QX200 ddPCR system consistently generated between 10 000 and 18 000 accepted droplets and the mean number of copies per droplets in our assays varied according to input DNA mass, to a maximum of 0.45 copies per droplet. To our knowledge, this manuscript complies with the essential requirements listed on the digital MIQE (Minimum Information for Publication of Quantitative Real-Time PCR Experiments) guidelines *(35)*.

Results

Using the QX200 ddPCR system with single hydrolysis probes targeting mutant alleles, we initially observed that droplets harboring a perfect complementary match between the probe and the targeted allele generated high fluorescence signal. Interestingly, probes in droplets with wild-type alleles were also consistently hydrolyzed, but at a much lower rate, because of the existence of base mispairings. This phenomenon allows direct counting of wild-type and mutant DNA molecules with one single probe and leads to the generation of distinct fluorescence amplitude bands following endpoint PCR, with the intrinsic lowest fluorescence emitted by empty droplets being the consequence of the imperfect quenching of uncleaved probes (Fig. 1). Herein, we leveraged this feature to implement a suite of uniplex and multiplexed ddPCR assays to detect and quantify clinically relevant mutations in B-cell lymphomas.

We first evaluated the performance of the hydrolysis probe targeting the *EZH2* Y641F mutation using an assay that lacked a probe targeting the wild-type allele on DNA from a cell line heterozygous for that mutation. The fractional abundance of each allele, as determined by counting intermediate droplets as wild-type molecules and top droplets as mutant molecules, was remarkably in line with the expectations derived from the analysis of a serial dilution of that cell line DNA (Fig. 2A). Moreover, we found a strong correlation between the VAFs inferred through this uniplex and a standard duplex assay that simultaneously targeted Y641F and wild-type alleles with probes labeled with different fluorophores ($r^2 = 0.991$, see online Supplemental Figs. 1 and 2). We designed probes targeting the remaining common *EZH2* and *STAT6* alleles and validated each through uniplex assays (i.e., no wild-type probes) on a set of liquid biopsies known to harbor different mutations [*(13, 34)*; also see online Supplemental Table 1]. We observed in all positive cases the generation of 3 fluorescent amplitude bands. We noted that up to 3 key factors played a critical role on the performance of single-probe assays: (*a*) annealing temperature (see online Supplemental Fig. 3), (*b*) the inclusion of an unlabeled oligonucleotide representing a wild-type version of the hydrolysis probe that competes for hybridization, and (*c*) probe and primer concentration (see online Supplemental Fig. 4).

The collection of 8 probes targeting recurrent somatic mutations at both *EZH2* and *STAT6* hotspots specifically reported the presence of mutant DNA in amounts as low as 0.05% in liquid biopsies and as low as 0.01% in highly diluted tumor DNA samples in one single reaction (see online Supplemental Fig. 5). We also tracked ctDNA levels in 5 patients enrolled in the Panobinostat trial from which liquid biopsies were available at 2 time points (day 0: start of the trial; day 15: 15 days after the start of the trial). The temporal trends of ctDNA abundance agreed with clinical observations. Each of 3 patients with stable disease upon their first clinical assessment following baseline exhibited a decrease in ctDNA from day 0 to day 15 (Fig. 3) *(34)*. This trend was not

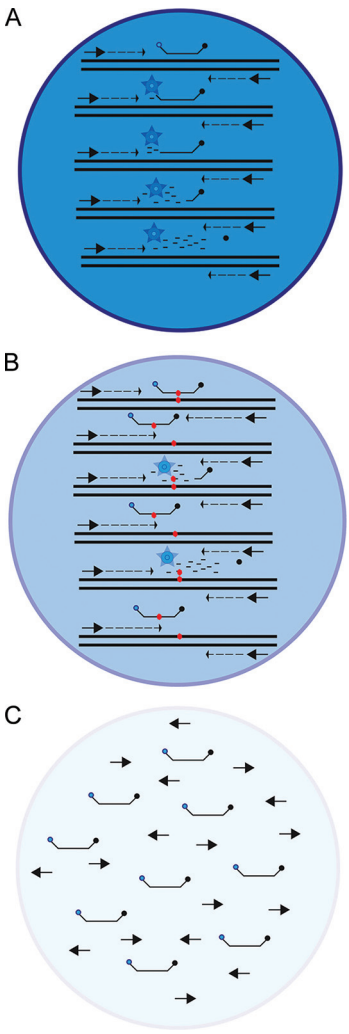

Fig. 1. Fundamentals of single hydrolysis probe-based assays.
The use of single fluorescent probes during ddPCR assays generated populations of droplets within at least 3 distinct and well-defined fluorescence amplitudes. The population of droplets showing the highest end-point fluorescence signal (A) was related to the specific and efficient cleavage of the probe during emulsion PCR. The population of droplets showing the lowest end-point fluorescence (C) was explained by the imperfect quenching of the fluorescent dye in droplets containing no template DNA. Interestingly, a second population of droplets exhibited an intermediate level of end-point fluorescence signal (B) caused by the unspecific and less efficient hydrolysis of the probe in the absence of a competing probe specifically targeting the allele that perfectly matches the DNA template. Large arrows denote PCR primers, blue and dark circles represent quenched fluorophores and molecular quenchers, respectively. Light blue stars represent active and free fluorophores. Single mismatches during the annealing of the probe and the DNA template (red dots) causes that the vast majority of probes get displaced instead of being hydrolyzed during PCR amplification.

observed in patients who relapsed on therapy, including a patient who showed an increased level of Y641H (Fig. 3) and a second patient (not shown in Fig. 3) who showed a marked increase in ctDNA, with a fractional abundance for *EZH2* Y641S >25% at day 15.

We next performed a series of titrations with varying probe concentrations such that the 4 probes targeting individual alleles of a hotspot would yield satisfactory separation in signal for each of *EZH2* (Fig. 4A) and *STAT6* (Fig. 4B). The resulting assays generated up to 6 well-defined fluorescence clusters when applied to a pool of DNAs harboring each of the 4 somatic mutations plus wild-type DNA. As expected, all samples known to harbor *EZH2* and *STAT6* mutations generated 3 clusters of droplets and only 2 clusters were observed in samples known to only harbor wild-type DNA (Fig. 4C, D; online Supplemental Fig. 6, online Supplemental Table 1). Particularly illustrative were the data obtained from the cell line carrying the heterozygous *EZH2* Y641F mutation [mutant allele: 33 copies/μL (Poisson maximum, minimum CIs, 36.4, 29.6); wild-type allele: 33.9 copies/μL (37.3, 30.5), Fig. 4D], for which the inferred abundance of each allele strongly fit expectations.

We then evaluated the performance of hydrolysis probes specifically targeting wild-type *EZH2* and *STAT6* alleles during uniplex ddPCR assays. Surprisingly, the generation of 3 different fluorescent bands allowed us to simultaneously count mutant and wild-type alleles with one single probe in 4 tumor DNA samples each known to harbor different *EZH2* mutations (Fig. 2). The investigation of the fractional distribution of alleles in the WSU-DLCL2 cell line DNA [wild-type copies/μL, 12.1 (14.0, 11.1); total copies/μL, 24.5 (27.3, 23.1)] together with a serial dilution of this DNA into a background of wild-type DNA supported the suitability of our inverted assay (Fig. 2). We then combined wild-type probes targeting *EZH2* and *STAT6* wild-type alleles, labeled with different fluorophores, to create an inverted assay for both hotspots (Fig. 5), and applied this to a series of fresh tumor and FFPE DNA samples with known mutations [*(15, 34)*; also see online Supplemental Table 1]. This assay accurately determined whether the samples harbored either an *EZH2* or *STAT6* mutation (or both) or whether samples were lacking mutations at either hotspot (see online Supplemental Fig. 7). Combining assays for each of the *MYD88* and *CCND3* hotspot mutations with mutant-specific probes revealed 2 fluorescence amplitude bands in the 6-FAM channel and 2 distinct fluorescence amplitude bands in the HEX channel (Fig. 6), allowing to count both mutant and wild-type molecules at the 2 loci in one single assay. This assay also accurately inferred whether a certain tumor sample carried a *MYD88* mutation or *CCND3* mutation or lacked mutations affecting either hotspot (see online Supplemental Table 1 and online Supplemental Fig. 8).

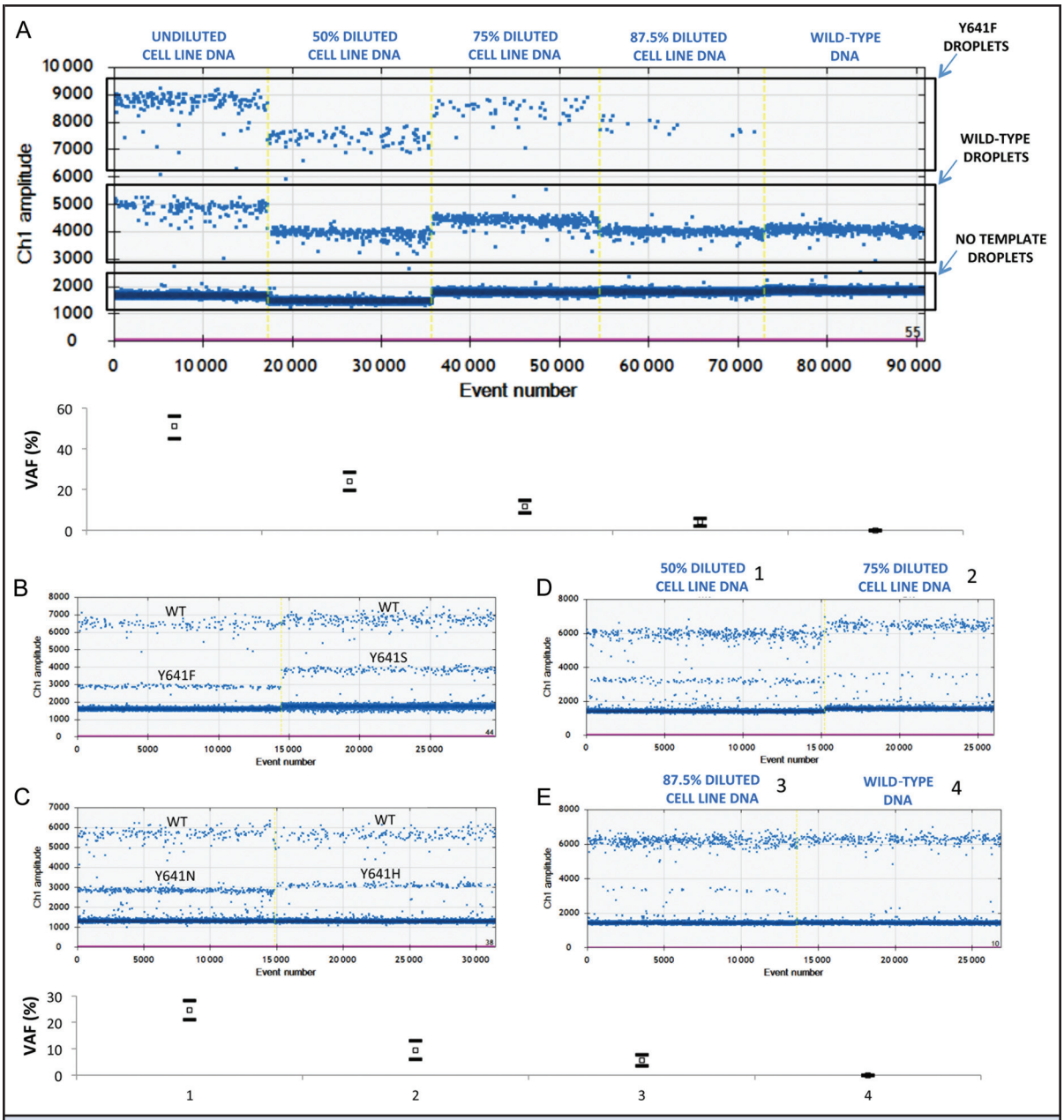

Fig. 2. Single hydrolysis probe-based assays on a QX200 ddPCR system.

Mutant allele quantification using a single hydrolysis probe targeting an *EZH2* Y641F mutation across a series of samples representing different dilutions of sheared cell line DNA heterozygous for that mutation in a background of nonfragmented wild-type DNA plus a pure sample of wild-type DNA used as negative control (A). Three different fluorescent amplitude bands can be observed for each assay, except for the wild-type DNA control (mutant droplets: top band, wild-type droplets: intermediate band; nontemplate droplets: bottom band). The chart below (A) shows the estimated fractional abundance of the mutant allele (white squares) together with Poisson maximum and minimum confidence intervals (horizontal black lines). Inverted ddPCR assays relying on hydrolysis probes matching wild-type sequences enabled the detection and quantification of multiple genetic aberrations (B and C). (D and E), Results derived from the analysis of a serial dilution of sheared WSU-DLCL2 cell line DNA in a background of nonfragment wild-type DNA (1 to 3), plus a pure sample of wild-type DNA (4). Three different fluorescent amplitude bands can be also observed for each assay, except for the wild-type negative control. The main particularity of inverted ddPCR assays was that mutant droplets were now within the intermediate top fluorescence amplitude band and wild-type droplets were within the top fluorescence amplitude band. The chart below displays VAFs estimates (white squares) and Poisson confidence intervals (horizontal black lines). Ch, channel.

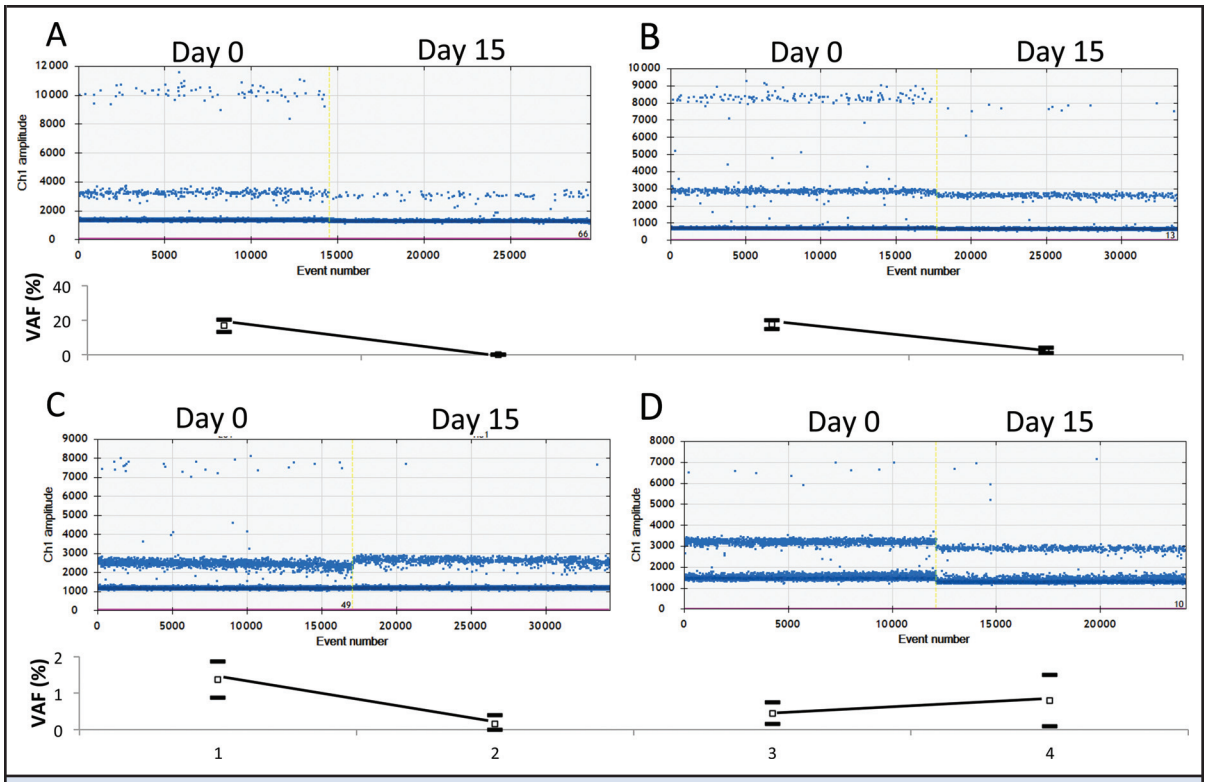

Fig. 3. Simultaneous quantification of wild-type and mutant DNA in a set of 4 paired liquid biopsy samples using hydrolysis probes targeting specific mutant alleles.

The fluorescence of droplets containing mutant molecules targeted by specific hydrolysis probes (upper fluorescence band) and wild type molecules (middle band) in 4 paired liquid biopsies drawn from DLBCL patients enrolled in a clinical trial testing the efficacy of the drug Panobinostat. The bottom band reflects empty droplets. Three of the cases shown exhibited response to the drug (A: targeting *STAT6* D419A, patient QC2–12; B: targeting *EZH2* Y641S, patient QC2–32; and C: targeting *EZH2* Y641S, patient QC2–15) and the fourth patient progressed despite treatment on this trial (D: targeting *EZH2* Y641H, patient QC2–07). White squares represent the estimated variant allele fraction (VAF) for mutant alleles and horizontal black lines delimit Poisson confidence intervals. Ch, channel.

Overall, the correlation between our ddPCR VAF estimates and the VAF estimates obtained through targeted hybrid capture coupled with next-generation sequencing *(13, 34)* was very high ($r^2 = 0.904$, n = 30; $P < 0.001$; see online Supplemental Fig. 2). We also observed strong concordance between the VAFs obtained through a duplex [15.9 copies/μL (19.1, 14.8)], uniplex [13.5 copies/μL (15.4, 11.6)] and an inverted ddPCR assay [16.9 copies/μL (18.1, 13.6)] conducted on the same FFPE tumor sample (patient QC2–02, see online Supplemental Table 1), in addition to the expected results every time that we tested different assays on the same cell line DNA sample (Figs. 2 and 4).

Discussion

We describe here a collection of accurate and versatile ddPCR assays with utility for screening tumor tissue or noninvasive genetic profiling of NHL patients, particularly focusing on mutations that are common and have potential clinical relevance in DLBCL and follicular lymphoma. Our custom probes targeting recurrent genetic alterations in *EZH2, STAT6, MYD88*, and *CCND3* have been validated for detection and quantification of somatic mutations in cell line DNA dilution series and clinical specimens representing fresh tumor, FFPE, and liquid biopsy samples. These probes could be applied in a wide variety of forms, including standard duplex hydrolysis probe-based assays. The main novelty of this study relies on the fact that our assays enable the simultaneous quantification of mutant and wild-type probes with one single probe. We also present multiplexed assays targeting mutation hotspots and the possibility to screen for mutations at 2 different loci in one single assay. A perceived disadvantage associated with forgoing specific probes during uniplex assays is the recognition of droplets with multiple templates. Wild-type counts could be therefore underestimated because the signal generated by

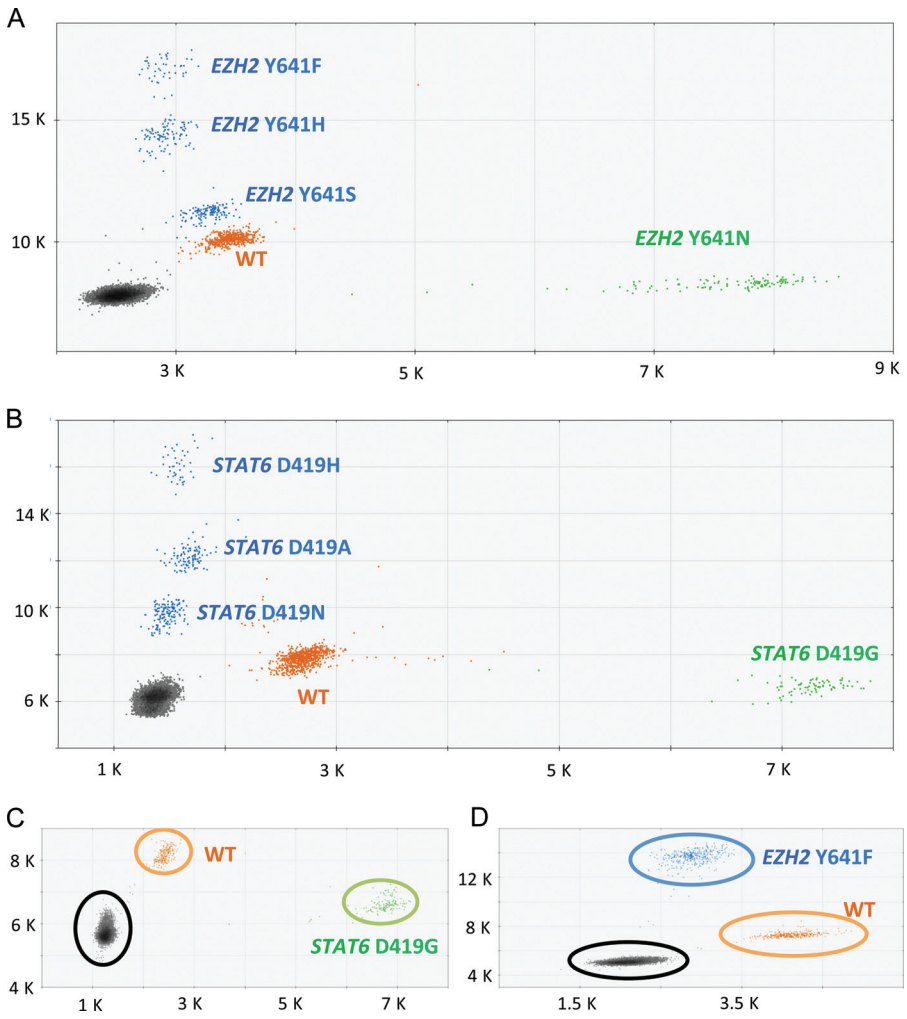

Fig. 4. Probe multiplexing for detecting mutations at *EZH2* Y641 and *STAT6* D419 lymphoma hotspots.

(A and B), a pool of DNA harboring different somatic mutations was interrogated with a pool of probes targeting up to 4 distinct nucleotide substitutions. Optimization of probe concentration translated into the generation of 6 unique fluorescence clusters: 1 for each targeted somatic mutation (3 blue and 1 green clusters), 1 for the wild-type (WT) alleles (large orange cluster), and another 1 just reflecting droplets with no DNA template (black cluster). Additional clusters (like the small orange cluster underneath the D419N text) is likely related to droplets containing a mixture of mutant (D419N in this case) and wild-type molecules. The use of these pools of probes over DNA carrying one specific mutation only generated 3 distinct clusters (C: sheared tumor DNA carrying a *STAT6* D419G mutation; D: WSU-DLCL2 cell line DNA carrying an *EZH2* Y641F mutation) one corresponding to mutant DNA, a second for wild-type DNA, and a third one for empty droplets. The *y* and *x* axes show fluorescence intensity units in the 6-FAM or HEX channel, respectively.

wild-type molecules might be obscured by the higher fluorescence signal generated by mutant molecules. This phenomenon would affect the VAF of mutant DNA, but because wild-type counts are only used as a denominator in VAF determination, the absolute count of mutant DNA molecules per microliter of sample would be unaffected. Droplets containing DNA molecules coming from different loci, on the contrary, would be easier to identify (Figs. 5 and 6).

To our knowledge, there are few published examples of multiplexed ddPCR assays pursuing hotspot mutations in cancer, and these typically focus on *KRAS (6)*. These studies targeted the 7 most common *KRAS* mutations in codons 12 and 13 across a cohort of plasma or FFPE samples obtained from colorectal cancer patients. Other multiplexed digital PCR designs have recently permitted researchers, for instance, to simultaneously target *ALK* (anaplastic lymphoma receptor tyrosine kinase),

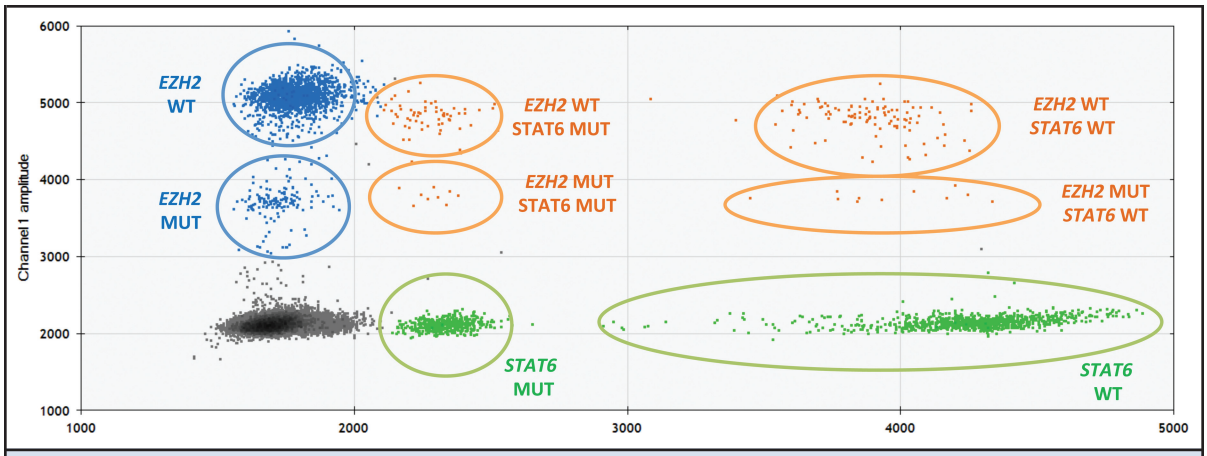

Fig. 5. Inverted ddPCR assay on a QX200 ddPCR system using 2 hydrolysis probes that target *EZH2* and *STAT6* wild-type (WT) alleles.

Nine different clusters can be noticed in this figure. The largest clusters of blue and green droplets are related to the specific hydrolysis of the probes inside droplets containing wild-type alleles. The nonspecific hydrolysis of wild-type probes, occurring in those droplets containing mutant DNA, accumulate lower fluorescence signal. These plots also permit elucidating the presence of droplets with mixed content based on the amount of relative fluorescence emitted in either the FAM or the HEX channel (orange circles). Empty droplets are depicted in black. MUT, mutant.

ROS1 (ROS proto-oncogene 1, receptor tyrosine kinase), and *RET* (ret proto-oncogene) fusions in lung cancer *(24)*. Such assays have been nevertheless developed for applications beyond cancer, including screening for variants associated with rare genetic disorders *(36)* and assessing the DNA integrity of clinical samples *(37)*. Similarly to the strong correlations that we found between ddPCR and NGS-based methods (see online Supplemental Fig. 2), the study by Taly et al. *(6)* also found strong correlations between the VAFs inferred independently by duplex and multiplex assays targeting the same mutations and the VAFs inferred through ddPCR and qPCR. It must be noted that we exclusively used fresh or FFPE tumor biopsies for a comparison between methods

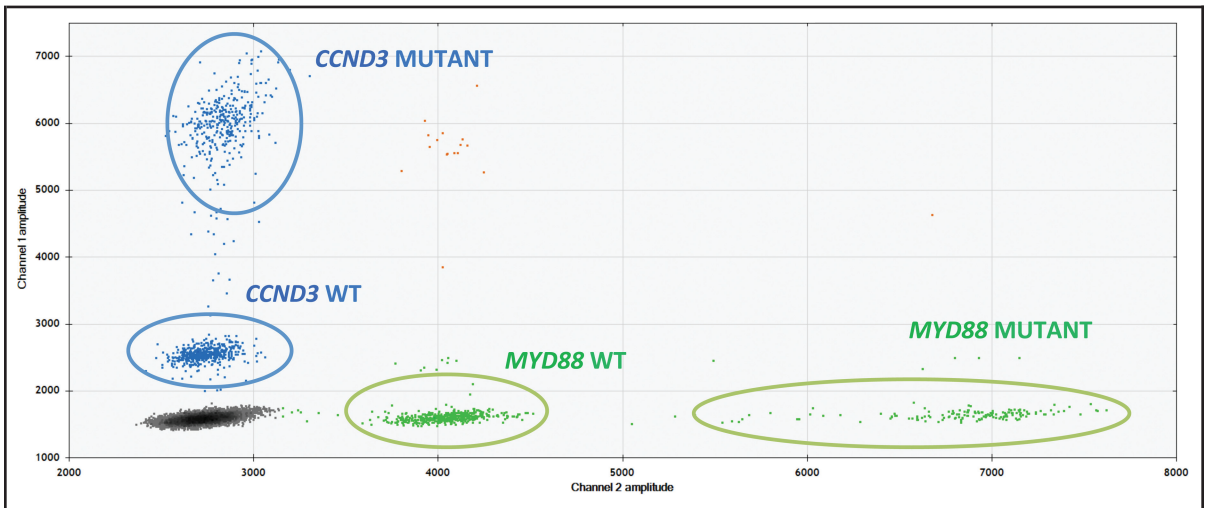

Fig. 6. Gene multiplexing on a QX200 ddPCR system using single hydrolysis probes that target specific single nucleotide variants.

The result from combining 2 probes, each targeting a distinct gene and labeled with different fluorophores (6-FAM: *CCND3* I290 hotspot; HEX: *MYD88* L265 hotspot). Two fluorescence amplitude bands were clearly generated for each gene (lower band: nonspecific hydrolysis of mutant probe; upper band: specific hydrolysis of mutant probe). Droplets presumably containing more than one template molecule are colored in orange. WT, wild type.

because we observed that ddPCR may underestimate the VAFs of mutant alleles if gDNA contamination from lysed cells has occurred during the storage and manipulation of blood samples. Whereas ddPCR counts gDNA fragments as wild-type fragments, the process of library preparation during NGS-based methods naturally removes these high molecular weight DNA fragments (unpublished data).

Previous studies have clearly demonstrated the enormous potential of ddPCR to detect minute amounts of ctDNA in plasma *(26, 30, 31)*. The analytical sensitivity of ddPCR has enabled researchers to monitor in the plasma, for instance, *BRAF* (B-Raf proto-oncogene, serine/threonine kinase) V600E, and epidermal growth factor receptor (*EGFR*) T790M mutations in melanoma and nonsmall lung cell lung cancer patients, respectively, at fractional abundances as low as 0.005% *(32, 38)*. Our uniplex assays have demonstrated outstanding analytical sensitivity by inferring mutant DNA levels as low as 0.01% in diluted tumor DNA samples and 0.05% in liquid biopsies in one single reaction (see online Supplemental Fig. 5). We believe uniplex and duplex assays may outperform multiplex assays relying on variable probe concentration in terms of analytical sensitivity owing to the potential difficulty to clearly discern between mutant and wild-type droplets when the mutant allele is targeted with the probe at the lowest concentration (Fig. 4) and shows a very low number of positives in the sample. A way to circumvent this potential issue would be using high concentration for all probes (e.g., 0.312 μmol/L or higher) during "blind" experiments (i.e., experiments in which mutations are not known a priori). This may enable a most confident identification of mutant DNA but it would require a second set of experiments to specify the exact nature of the mutation and it will also consume more probes.

The collection of assays presented here offers diverse opportunities to balance cost and scope against accuracy for applications to tissue or ctDNA. As we have done, we expect that the multiplex assays will be typically used in screening tissue samples for common hotspots, and subsequent uniplex assays matching the identified allele would be used for corresponding ctDNA samples. Though inverted ddPCR assay hold promise for the detection of rare mutations in fresh tumor and FFPE biopsies with VAFs around 10% and higher (Fig. 2), we believe their analytical sensitivity on ctDNA might be compromised by high false-positive rates. Amplification efficiency can differ between droplets due to factors such as the presence of PCR inhibitors, probe performance or the pattern of DNA fragmentation; hence, droplets containing wild-type alleles could be mistaken with droplets containing mutant alleles. We nonetheless assert that inverted assays could offer an alternative for detecting rare germline mutations causing genetic disorders. However, probe efficiency in other situations such as indels or complex mutations requires further exploration. Access to samples displaying such genetic alterations for a proper validation is challenging. A recently published study by Castellano-Rizaldos et al. *(25)* also used wild-type probes for mutation scanning experiments. Their method is based on a combination of COLD (coamplification at lower denaturation temperature)-PCR with ddPCR using 2 FAM/HEX probes targeting 2 wild-type sequences in the locus of interest. One advantage of this method over our inverted ddPCR is that Castellano-Rizaldo et al. demonstrated sensitivity levels as low as 0.2% for *TP53* and *EGFR* mutations and can cover longer stretches of one particular locus. In contrast, the main advantage of our method is the ability to perform mutation scans at 2 different genes in one single experiment.

In summary, this study extends the benefits of ddPCR to the genetic profiling and noninvasive assessment of common forms of NHLs. The ddPCR-based assays reported here should enhance the early diagnosis, prognostication, and therapeutic management of common B-cell lymphomas. The field of personalized medicine *(39, 40)* demands patient-specific molecular assays to track ctDNA levels in the blood or other biological fluids *(26)*. We assert that the single-probe strategy introduced here may enable researchers and clinicians to design cost-effective experiments that demand lower amounts of clinically precious samples and, notably, promote the possibility to investigate clonal evolution in response to therapeutic treatment by tracking multiple mutations in one single assay.

Author Contributions: *All authors confirmed they have contributed to the intellectual content of this paper and have met the following 3 requirements: (a) significant contributions to the conception and design, acquisition of data, or analysis and interpretation of data; (b) drafting or revising the article for intellectual content; and (c) final approval of the published article.*

Authors' Disclosures or Potential Conflicts of Interest: *Upon manuscript submission, all authors completed the author disclosure form. Disclosures and/or potential conflicts of interest:*

Employment or Leadership: None declared.
Consultant or Advisory Role: None declared.
Stock Ownership: None declared.
Honoraria: None declared.
Research Funding: N.A. Johnson, the Jewish General Hospital Foundation; R.D. Morin, the Canadian Institute for Health Research (CIHR) New Investigator award and operating grant 300738, the Terry Fox Research Institute (#1043 and #1021), the Natural Sciences and Engineering Research Council of Canada (Research Tools and Instruments program EQPEQ 1501), and the BC Cancer Foundation.
Expert Testimony: None declared.
Patents: None declared.

Role of Sponsor: The funding organizations played a direct role in the design of study, choice of enrolled patients, review and interpretation of data, preparation of manuscript, and final approval of manuscript.

Acknowledgments: We thank anonymous reviewers for their helpful and constructive comments on a previous version of this manuscript.

References

1. Crowley E, Di Nicolantonio F, Loupakis F, Bardelli A. Liquid biopsy: monitoring cancer-genetics in the blood. Nat Rev Clin Oncol 2013;10:472–84.
2. Kurtz DM, Green MR, Bratman SV, Scherer F, Liu CL, Kunder CA, et al. Noninvasive monitoring of diffuse large B-cell lymphoma by immunoglobulin high-throughput sequencing. Blood 2015;125:3679–87.
3. Heitzer E, Auer M, Ulz P, Geigl JB, Speicher MR. Circulating tumor cells and DNA as liquid biopsies. Genome Med 2013;5:73.
4. Karachaliou N, Mayo-de-las-Casas C, Molina-Vila MA, Rosell R. Real-time liquid biopsies become a reality in cancer treatment. Ann Transl Med 2015;3:36.
5. Lièvre A, Bachet J, Corre D Le, Landi B, Ducreux M, Rougier P. *KRAS* mutation status is predictive of response to cetuximab therapy in colorectal cancer. Cancer Res 2006;66:3992–5.
6. Taly V, Pekin D, Benhaim L, Kotsopoulos SK, Le Corre D, Li X, et al. Multiplex picodroplet digital PCR to detect *KRAS* mutations in circulating DNA from the plasma of colorectal cancer patients. Clin Chem 2013;59:1722–31.
7. Morin RD, Gascoyne RD. Newly identified mechanisms in B-cell non-Hodgkin lymphomas uncovered by next-generation sequencing. Semin Hematol 2015;50:303–13.
8. Morin RD, Johnson NA, Severson TM, Mungall AJ, An J, Goya R, et al. Somatic mutations altering *EZH2* (Tyr641) in follicular and diffuse large B-cell lymphomas of germinal-center origin. Nat Genet 2010;42:181–5.
9. Bödör C, Grossmann V, Popov N, Okosun J, O'Riain C, Tan K, et al. EZH2 mutations are frequent and represent an early event in follicular lymphoma. Blood 2013;122:3165–8.
10. McCabe MT, Ott HM, Ganji G, Korenchuk S, Thompson C, Van Aller GS, et al. EZH2 inhibition as a therapeutic strategy for lymphoma with EZH2-activating mutations. Nature 2012;492:108–12.
11. Bradley WD, Arora S, Busby J, Balasubramanian S, Gehling VS, Nasveschuk CG, et al. EZH2 inhibitor efficacy in non-Hodgkin's lymphoma does not require suppression of H3K27 monomethylation. Chem Biol 2014;21:1463–75.
12. Yildiz M, Li H, Bernard D, Amin NA, Ouillette P, Jones S, et al. Activating *STAT6* mutations in follicular lymphoma. Blood 2014;125:668–79.
13. Morin RD, Assouline SE, Alcaide M, Mohajeri A, Johnston RL, Chong L, et al. Genetic landscapes of relapsed and refractory diffuse large B cell lymphomas. Clin Cancer Res 2015;22:2290–300.
14. Kim Y, Ju H, Kim DH, Yoo HY, Kim SJ, Kim WS, Ko YH. CD79B and *MYD88* mutations in diffuse large B-cell lymphoma. Hum Pathol 2014;45:556–64.
15. Kraan W, van Keimpema M, Horlings HM, Schilder-Tol EJ, Oud ME, Noorduyn LA, et al. High prevalence of oncogenic *MYD88* and *CD79B* mutations in primary testicular diffuse large B-cell lymphoma. Leukemia 2014;28:719–20.
16. Poulain S, Roumier C, Decambron A, Renneville A, Herbaux C, Bertrand E, et al. M*YD88* L265P mutations in Waldenstrom's macroglogulinemia. Blood 2013;121:4504–11.
17. Wilson WH, Young RM, Schmitz R, Yang Y, Pittaluga S, Wright G, et al. Targeting B cell receptor signaling with ibrutinib in diffuse large B cell lymphoma. Nat Med 2015;21:922–6.
18. Bohers E, Mareschal S, Bouzelfen A, Marchand V, Ruminy P, Maingonnat C, et al. Targetable activating mutations are very frequent in GCB and ABC diffuse large B-cell lymphoma. Genes Chromosomes Cancer 2014;53:144–53.
19. Gunawardana J, Chan FC, Telenius A, Woolcock B, Kridel R, Tan KL, et al. Recurrent somatic mutations of *PTPN1* in primary mediastinal B cell lymphoma and Hodgkin lymphoma. Nat Genet 2014;46:329–35.
20. Marusyk A, Polyak K. Tumour heterogeneity: causes and consequences. Biochim Biophys Acta 2010;1805:105–17.
21. Li P, Gu J, Yang X, Cai H, Tao J, Yang X, et al. Functional promoter -94 ins/del ATTG polymorphism in *NFKB1* gene is associated with bladder cancer risk in a Chinese population. PLoS One 2013;8:e71604.
22. Mekenkamp LJ, Tol J, Dijkstra JR, de Krijger I, Vink-Börger ME, van Vliet S, et al. Beyond KRAS mutation status: influence of *KRAS* copy number status and microRNAs on clinical outcome to cetuximab in metastatic colorectal cancer patients. BMC Cancer 2012;12:292.
23. Persson M, Andren Y, Mark J, Horlings HM, Persson F, Stenman G. Recurrent fusion of *MYB* and *NFIB* transcription factor genes in carcinomas of the breast and head and neck. Proc Natl Acad Sci U S A 2009;106:18740–4.
24. Lira ME, Choi YL, Lim SM, Deng S, Huang D, Ozeck M, et al. A single-tube multiplexed assay for detecting *ALK,* ROS1, and RET fusions in lung cancer. J Mol Diagn 2014;16:229–43.
25. Castellanos-Rizaldos E, Paweletz C, Song C, Oxnard GR, Mamon H, Jänne PA, Makrigiorgos GM. Enhanced ratio of signals enables digital mutation scanning for rare allele detection. J Mol Diagn 2015;17:284–92.
26. De Mattos-Arruda L, Mayor R, Ng CKY, Weigelt B, Martínez-Ricarte F, Torrejon D, et al. Cerebrospinal fluid-derived circulating tumour DNA better represents the genomic alterations of brain tumours than plasma. Nat Commun 2015;6:8839.
27. Elshimali Y, Khaddour H, Sarkissyan M, Wu Y, Vadgama J. The clinical utilization of circulating cell free DNA (CCFDNA) in blood of cancer patients. Int J Mol Sci 2013;14:18925–58.
28. Forshew T, Murtaza M, Parkinson C, Gale D, Tsui DW, Kaper F, et al. Noninvasive identification and monitoring of cancer mutations by targeted deep sequencing of plasma DNA. Sci Transl Med 2012;4:136ra68–ra136ra68.
29. Zeerleder S. The struggle to detect circulating DNA. Crit Care 2006;10:142.
30. Garcia-Murillas I, Schiavon G, Weigelt B, Ng C, Hrebien S, Cutts RJ, et al. Mutation tracking in circulating tumor DNA predicts relapse in early breast cancer. Sci Transl Med 2015;7:302ra133–ra302ra133.
31. Kinugasa H, Nouso K, Tanaka T, Miyahara K, Morimoto Y, Dohi C, et al. Droplet digital PCR measurement of *HER2* in patients with gastric cancer. Br J Cancer 2015;112:1652–5.
32. Sanmamed MF, Fernandez-Landazuri S, Rodriguez C, Zárate R, Lozano MD, Zubiri L, et al. Quantitative cell-free circulating BRAFV600E mutation analysis by use of droplet digital PCR in the follow-up of patients with melanoma being treated with BRAF inhibitors. Clin Chem 2015;61:297–304.
33. Morin RD, Mungall K, Pleasance E, Mungall AJ, Goya R, Huff RD, et al. Mutational and structural analysis of diffuse large B-cell lymphoma using whole-genome sequencing. Blood 2013;122:1256–65.
34. Assouline S, Nielsen TH, Yu S, Alcaide M, Chong L, MacDonald D, et al. Phase 2 study of panobinostat +/− rituximab in relapsed diffuse large B cell lymphoma and biomarkers predictive of response. Blood 2016;128:185–94.
35. Huggett JF, Foy CA, Benes V, Emslie K, Garson JA, Haynes R, et al. The digital MIQE guidelines: Minimum Information for Publication of Quantitative Digital PCR Experiments. Clin Chem 2013;59:892–902.
36. Zhong Q, Bhattacharya S, Kotsopoulos S, Olson J, Taly V, Griffiths AD, et al. Multiplex digital PCR: breaking the one target per color barrier of quantitative PCR. Lab Chip 2011;11:2167–74.
37. Didelot A, Kotsopoulos SK, Lupo A, Pekin D, Li X, Atochin I, et al. Multiplex picoliter-droplet digital PCR for quantitative assessment of DNA integrity in clinical samples. Clin Chem 2013;59:815–23.
38. Watanabe M, Kawaguchi T, Isa S, Ando M, Tamiya A, Kubo A, et al. Ultra-sensitive detection of the pretreatment *EGFR* T790M mutation in non-small cell lung cancer patients with an *EGFR*-activating mutation using droplet digital PCR. Clin Cancer Res 2015;21:3552–60.
39. Cho S-H, Jeon J, Kim S Il. Personalized medicine in breast cancer: a systematic review. J Breast Cancer 2012;15:265–72.
40. Lili LN, Matyunina LV, Walker LD, Daneker GW, McDonald JF. Evidence for the importance of personalized molecular profiling in pancreatic cancer. Pancreas 2014;43:198–211.